Scientia Iranica A (2015) 22(4), 1435–1448

Sharif University of Technology
Scientia Iranica
Transactions A: Civil Engineering
www.scientiairanica.com

Impact of solar radiation on the uncoupled transient thermo-structural response of an arch dam

H. Mirzabozorg[a], M.A. Hariri-Ardebili[b,*] and M. Shirkhan[a]

a. *Department of Civil Engineering, K.N. Toosi University of Technology, Tehran, Iran.*
b. *Department of Civil Environmental and Architectural Engineering, University of Colorado, Boulder, USA.*

Received 19 January 2014; received in revised form 7 October 2014; accepted 15 November 2014

KEYWORDS
Arch dam;
Solar radiation;
Thermo-structural;
Uncoupled transient analysis;
Seismic;
Finite element.

Abstract. In this paper, the impact of solar radiation on the uncoupled transient thermo-structural behavior of an arch dam was investigated under the earthquake loading. Temperature distribution within the dam body was determined by solving the governing differential equations taking into account the water and air temperature and the solar radiation. Finite element model of the dam-reservoir-foundation system including joint nonlinearity was excited using three-component ground motion. Results of the thermal transient analysis with and without solar radiation effects were used as an initial boundary condition for the seismic analysis. Results showed that considering solar radiation leads to non-uniform temperature distribution on the exposed faces and increasing the tensile stresses within the dam body.

1. Introduction

Thermal loads play an important role in structural behavior of thin arch dams due to high thermal gradient between the upstream and downstream faces. The thermo-structural models can be categorized in three main groups: (1) Uncoupled model in which the transient thermal analysis is performed first, and the corresponding thermal stresses and strains are computed using the temperature-independent mechanical properties of the concrete. Transient fluid-structure interaction is then performed using the results of the thermal transient analysis as initial conditions; (2) Weakly coupled model in which the structural analysis is performed using temperature-dependent material properties for concrete; (3) Strongly coupled model in which the thermal transient analysis is repeated between each step of structural analysis using the updated data.

Based on the USACE recommendations [1], thermal study for arch dams falls into two categories: (1) The operational temperature study and, (2) The construction temperature study. The operational temperature studies are related to determination of the temperature distributions that the dam will experience during its expected life time. Specifically temperature distribution in air, reservoir, foundation and the solar radiation are of interest. The construction temperature studies are usually performed, after an acceptable layout has been obtained. The construction temperature studies are needed to assure that the design closure temperature can be obtained while minimizing the possibility of thermally induced cracking.

The temperature effect may be considered in various phases of design. Arch dam design is usually completed in three main phases [1]:

1. Reconnaissance: No detailed design is required.

*. *Corresponding author. Tel.: +1 3039902451*
E-mail addresses: mirzabozorg@kntu.ac.ir (H. Mirzabozorg); mohammad.haririardebili@colorado.edu (M.A. Hariri-Ardebili); shirkhan@sina.kntu.ac.ir (M. Shirkhan)

Only the site selection and the dam's concrete volume computation are performed.

2. Feasibility: Limited design work should be accomplished. The preliminary load combinations should be established and the temperature loading on the dam should be estimated from a study of similar projects.
3. Pre-construction engineering and design: Detailed design and analysis of the dam are to be performed. The temperature loading needs to be determined from the results of the temperature study which is initiated at beginning of this phase.

Early 1950s researchers began to study the effect of solar radiation on dam surfaces. Tarbox [2] presented charts showing the temperature increase resulting from solar radiation. ICOLD [3] published a report on deterioration of dams and reservoirs and listed freezing/thawing and external temperature variations as the most common cause of deterioration in concrete dams. Some researchers have shown the significant role of the thermal cyclic stresses in degradation of the strength and stiffness of concrete dams located at the Quebec province [4-6]. NRC [7] declared that the available strain capacity to resist the seismic induced forces without concrete damage is affected by various factors like the season at which the earthquake occurs. Leger et al. [8] studied the importance of the temperature variations and the associated thermal stresses as the initial loading conditions for safety evaluation of gravity dams.

Meyer and Mouvet [9] investigated thermal behavior of Vieux-Emosson arch-gravity dam in Switzerland using finite element method. They found that the air temperature, fluctuation is not a lonely good criterion for estimation of concrete dam temperature, and solar radiation increases the whole dam temperature of about 4°C. Agullo et al. [10] presented a numerical model based on explicit finite difference method to measure the temperature of concrete dam subjected to environmental thermal action during operation stages. They used energy conversion factor for radiation modeling and Newton's law for simulation of thermal convection. Zhang and Garga [11] assumed a unidirectional heat transfer and applied a new analytical method to determine the temperature distribution and thermal stress in mass concrete structures subjected to thermal shock. They found that the highest temperature gradient is induced in a very thin region close to the exposed surface; the stress concentration can be reduced by changing the property of concrete and heat transfer coefficient as a curing condition.

Chen et al. [12] developed a 3D finite element relocating mesh method for thermal analysis and determination of the stress distribution in a RCC dam during the construction period. Sheibany and Ghaemian [13] proposed a 3D finite element model to study the thermal stresses on Karaj arch dam. Spatial variations in solar radiation across the entire exposed surface of the dam were considered. The results showed that the thermal loads have a significant role in initiating downstream cracks in comparison with self-weight and hydrostatic loads. The cracking areas were consistent with the regions corresponding to high temperature associated with solar radiation. However, the shade effects of surrounding terrain were not considered. Noorzaei et al. [14] developed a 2D finite-element code for thermal and structural analysis of RCC dams. They considered the actual climatic conditions and thermal properties of Kinta RCC dam. Computed temperatures from the numerical analysis were in a good agreement with the actual temperatures measured by the thermocouples installed within the dam body. Jaafar et al. [15] developed a finite element code to determine the temperature distribution within the dam body to investigate the effects of thermal stresses on RCC dams. They applied the developed model to a real-scale problem and found that for a given RCC dam, changing the placing schedule can optimize the location of maximum temperature zones.

Leger and Seydou [16] investigated the displacement value due to the effect of seasonal temperature, and compared it with the recorded displacement by pendulum measurements on a real 40 m gravity dam located. They presented 1D and 2D finite element hybrid dam displacement model to interpret these displacements and to extrapolate the response for extreme thermal events. Jin et al. [17] presented a practical model for predicting the non-uniform temperature distribution on the exposed faces of arch dams considering combination of the ASHRAE (American Society of Heating, Refrigerating and Air Conditioning Engineers) clear sky model for solar radiation effects and the ray-tracing algorithm to consider the shade effects on 240 m high parabolic double-curvature Ertan arch dam. They showed that the computed temperatures are in good agreement with the measured ones and the solar radiation leads to the non-uniform temperature distribution on the downstream face of the dam. Chen et al. [18] developed an algorithm for thermal analysis of massive concrete specimen with lift joints based on the composite element method. Yang et al. [19] developed a 3D finite element program for thermal analysis of mass concrete embedded with double-layer staggered heterogeneous cooling water pipes based on the equivalent equation of heat conduction including the effect of cooling water pipes and hydration heat of concrete. Comparing calculated results with the actual measured data from a monolith of an arch dam in China, their numerical model was proven to be effective in sufficiently simulating accurate temperature variations of mass concrete. Yangbo et al. [20] proposed

two fast algorithms to overcome the huge finite element model, complex environmental conditions and time-consuming process of simulation analysis solution on temperature control and thermal stress fields of concrete dams' construction. One was the overall planning algorithm and the other was the incomplete Cholesky conjugate gradient algorithm. Fujun et al. [21] studied the cracking reasons for concrete overflow dam of Hadashan Hydro Project by developing a 3D finite element method to simulate temperature analysis and thermal stress distribution during the construction period. They showed that the crack of the concrete overflow dam was temperature crack due to combined action of the internal thermal gradient and the external restraints. Sabbagh-Yazdi and Amiri-SaadatAbadi [22] computed variation of material properties due to varying temperature generated by cement hydration using 2D matrix free Galerkin finite volume. They modeled time-dependent thermal stress profiles during gradual construction of a concrete dam. Kuzmanovic et al. [23] proposed a new approach for 3D numerical modeling of unsteady phased thermal-stress analysis of a massive concrete hydraulic structure which could be used for the unsteady, nonlinear, viscoelastic stress-strain analysis. They verified the proposed model based on the field investigations of the Platanovryssi dam. Hu et al. [24] developed an external thermal model including five types of external heat flux, i.e. air-side convection, electromagnetic radiation, absorbed solar input, water-side convection, and surface insulation effect. They proposed a method based on Boolean operations for extracting the external surfaces of dams. They implemented the proposed model on a high arch dam and found that it is able to correctly estimate the monitored responses. Maken et al. [25] evaluated the thermo-mechanical behavior of a gravity dam and an arch dam. No seismic analysis was performed. Only the temperature-dependent behavior of material was investigated. They found that it is conservative to consider the variation in mechanical properties of concrete with temperature (in particular, the increase in tensile strength). However, from a practical standpoint, the difference is not very significant. It means that the temperature-dependent material properties can be neglected in analysis and constant value might be assumed for material characteristics. Mirzabozorg et al. [26] investigated the solar radiation effects on thermal transient analysis of a thin arch dam. They found that the solar radiation has an important role on non-uniform temperature distribution with the dam body. However, they did not study the thermal-induced stresses.

In summary, it should be mentioned that the thermal issues in massive concreting are one of the main challenges during construction stage because large amount of concreting leads to a very slow heat exchange between the material and the environment. Consequently, high temperature and stress within the dam body may lead to concrete deterioration. Thermal loads should be considered both in design and analysis of arch dams. The impact of thermal loads is more significant in static analysis; however, under the dynamic loads, the interaction of the thermal and seismic stresses might also be important.

On the other hand, many of the aforementioned researches highlighted the impact of the solar radiation on thermal analysis of massive concrete specimen especially when the temperature gradient is significant.

The contribution of the authors, in the present paper, is to combine the transient thermal analysis and the nonlinear dynamic analysis for proper assessment of a thin arch dam. The impact of solar radiation is also investigated in thermal transient analysis. The thermal induced stresses (with and without solar radiation effect) are computed and combined with the stresses due to self-weight, hydrostatic pressure and the seismic excitation. In the performed structural analyses, the contraction and peripheral joints are also modeled.

2. Thermal transient analysis

2.1. Heat transfer problem

Thermal conduction is due to temperature gradient and is formulated based on the principle of thermal energy conservation [26]:

$$\rho C \frac{\partial T}{\partial t} = \text{div}\left(\vec{k}\ \text{grad}\ T\right) + Q, \tag{1}$$

where, ρ is density, C is specific heat, T is temperature of medium, t is time, $\vec{k}$ is a tensor representing thermal conduction coefficient, and Q is internal heat generated per volume.

The amount of heat transferred by convection is modeled using Newton's cooling law given as:

$$q_c = -h_c(T_a - T_{sb}), \tag{2}$$

where, h_c is convection coefficient, T_{sb} is temperature of surface boundaries, and T_a is ambient temperature. Convection coefficient is a function of fluid velocity (wind speed in this case), V_f, and its properties such as type of flow and viscosity. This parameter may be computed by the following equation proposed by McAdams [27]:

$$h_c = 3.8V_f + 5.7. \tag{3}$$

Thermal radiation is a type of electromagnetic emission. Every object hotter than absolute zero emits electromagnetic waves with capability of transferring energy. Radiation energy may be absorbed by or emitted from surfaces. The total amount of absorbed

energy may be expressed by [8]:

$$q_a = aI_t, \tag{4}$$

where, a is solar absorptivity of surface, and I_t is total solar energy on surface. Thermal radiation caused by the temperature difference between surface and its environment can be achieved by Stefan-Boltzman law [7]:

$$q_r = -eC_s\left(T_a^4 - T^4\right), \tag{5}$$

where, e is emissivity of surface that is the ratio of heat released by intended surface to heat released by a black body with the same temperature, and $C_s = 5.669 \times 10^{-8}$ $\mathrm{Wm^{-2}K^{-4}}$ is Stefan-Boltzman constant. It should be noted that the wasted heat between the surface and air due to radiation is not significant. Thus, Eq. (5) can be rewritten as a pseudo-linear equation as:

$$q_r = -\underbrace{eC_s\left(T_a^2 + T^2\right)(T_a + T)}_{h_r}(T_a - T). \tag{6}$$

Therefore, the radiation effects can be considered by adding h_r to h_c and obtaining new convective coefficient.

2.2. Thermal boundary conditions

Boundary conditions of a generic 3D arch dam for the heat transfer differential equation are shown schematically in Figure 1. These conditions include imposed temperature, imposed heat flux and convection through the peripheral nodes. Figure 2 summarizes the general procedure for heat transfer boundary conditions implemented in the finite element model in order to analyze thermal transient. Estimation of the air temperature at the dam site usually depends on the data obtained from the nearest weather stations. In the current study, appropriate data were collected from weather stations including the (maximum, minimum and mean) monthly temperature, the annual temperature, and the highest and lowest recorded temperatures [26]. The dam body temperature is strongly affected by the reservoir temperature. The best source for this information is the collected statistical data from similar reservoirs. This type of information is collected by USBR and reported in engineering supplement no. 34 [28]. The proposed method by Bofang [29] is another technique for determination of the reservoir temperature that is used in the present study.

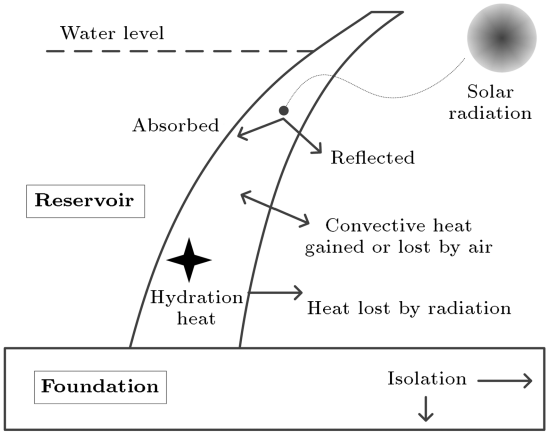

Figure 1. Heat transfer mechanism for an arch dam.

As discussed by Mirzabozorg et al. [26], temperature rising on the exposed surface due to solar radiation depends on the slope, direction, and latitude of the surface with respect to sun. The navigation of all parts of the gravity dams are similar and only one value for each side of the dam body would be required while for an arch dam this value should be calculated for more points with respect to its shape. The amount of solar radiation received by a concrete arch dam follows a series of periodic seasonal changes. This variation is a function of different factors such as the elevation of the dam site with respect to the sea level, surface directions relative to sun, surface slop relative to horizon, the regional cloud cover, surrounding topography of the dam site, and the time of the year. Figure 3 shows the procedure for implementation of the solar radiation in the finite element code. In this figure, total solar energy received on an inclined surface, I_t, is computed based on the total days that the solar is radiated on the horizontal surface, D; daily diffused solar radiation on horizontal surface, D_d; the diffuse reflectance coefficient of the surrounding surface, ρ_d; and the ratio of direct radiation on the inclined surface to the horizontal surface, R_b. The Angstrom equation [30] can be used to get the amount of in place sunny hours where a and b are experimental constants depended on geographical location of the dam, and the parameter n' is mean monthly sunny hour in the station. D_0 is monthly extra-terrestrial radiation on horizontal surface which depends on solar constant, G_{sc}; and the number of the day in A.D. year, n. The parameter ϕ is the angular position of the given surface to the equator; δ is the angular position of the sun at the solar noon to the equator; γ is the surface azimuth angel; and β is the angel between the given surface and the horizon.

2.3. Finite element implementation

In the present study, finite element technique is used for numerical implementation of the heat transfer problem within the dam. The mathematical description of heat transfer relation for a system including anisotropic material in 3D space was explained in Eq. (1). The general equation for transient heat transfer problem can be written as [31]:

$$\left[C^{(e)}\right]\left\{\dot{T}^{(e)}\right\} + \left[K^{(e)}\right]\left\{T^{(e)}\right\} = \left\{f_Q^{(e)}\right\} + \left\{f_q^{(e)}\right\}, \tag{7}$$

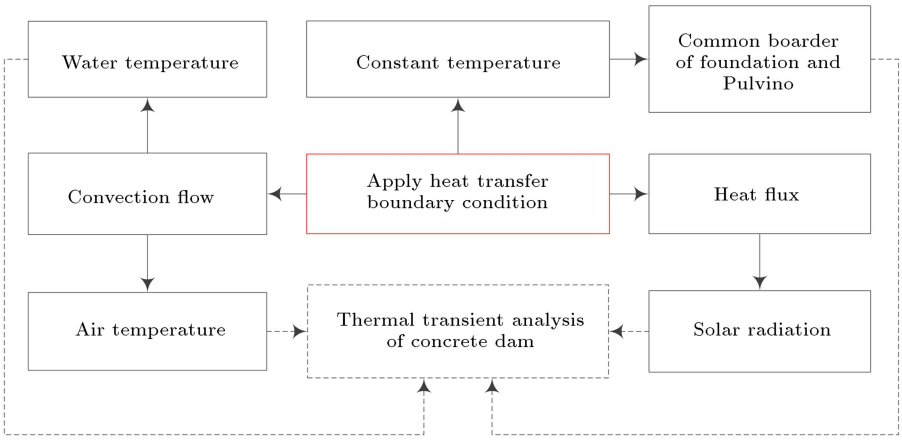

Figure 2. Implementation of the heat transfer boundary conditions for dam.

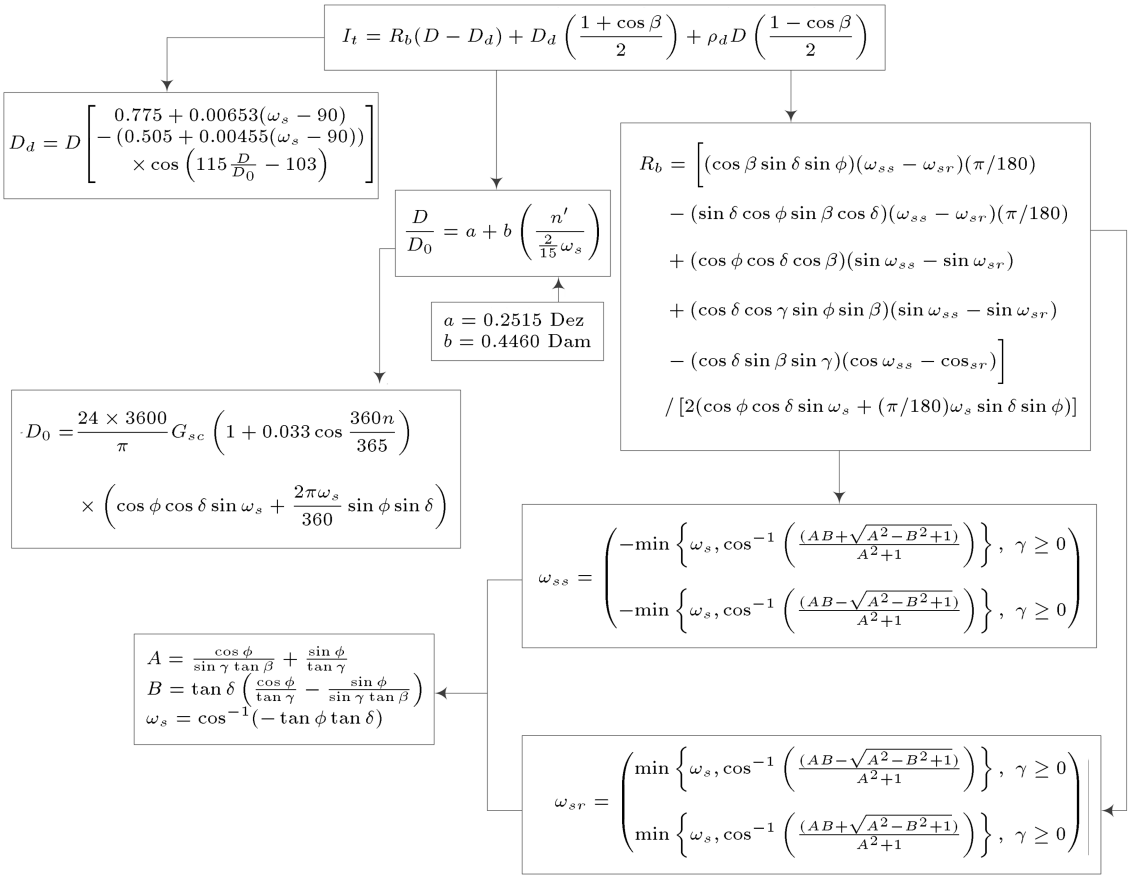

Figure 3. Calculation of the total solar energy received on an inclined surface.

where $\left\{\dot{T}^{(e)}\right\}$ is temperature vector, $\left[C^{(e)}\right]$ is element conspecific heat matrix, $\left[K^{(e)}\right]$ is element conductivity matrix, $\left\{f_Q^{(e)}\right\}$ is element heat generation vector, and $\left\{f_q^{(e)}\right\}$ is element convection surface heat flow vector, and all are defined as:

$$\left[K^{(e)}\right] = \iiint_V \left[k_x\frac{\partial[N]^T}{\partial x}\frac{\partial[N]}{\partial x} + k_y\frac{\partial[N]^T}{\partial y}\frac{\partial[N]}{\partial y} + k_z\frac{\partial[N]^T}{\partial z}\frac{\partial[N]}{\partial z}\right]dV, \tag{8}$$

$$\left[C^{(e)}\right] = \iiint_V \rho c[N][N]^T dV, \tag{9}$$

$$\left\{f_Q^{(e)}\right\} = \iiint_V Q[N]^T dV, \tag{10}$$

$$\left\{f_q^{(e)}\right\} = -\iint_A \left(k_x \frac{\partial T}{\partial x} n_x + k_y \frac{\partial T}{\partial y} n_y + k_z \frac{\partial T}{\partial z} n_z\right)[N][N]^T dA, \quad (11)$$

where n_x, n_y and n_z are unit normal vectors on the considered surface, k_x, k_y and k_z are conduction coefficients of mass concrete in x, y and z global directions, respectively, and $[N]$ is the shape function of the thermal element.

3. Illustrative example

3.1. Case study description

Dez Dam is one of the tallest arch dams in Iran. This dam was built in south-west of Iran, in the Khuzestan province and on Dez River [32]. Location coordinates are: Latitude = 32.6053 and Longitude = 48.464. Dez is a double-curvature thin arch dam. Its height is 203 m from the foundation and 190 m from the river-bed. The thickness is 4.5 m at the crest and 27 m at the base of the crown cantilever. The dam crest length is 212 m and the crest elevation is 354 m above sea level (asl). The maximum operation level of the reservoir was designed at 350 m asl. In order to optimize operation, it was increased to the level of 352 m asl, since 1980. A concrete Pulvino has been implemented between the concrete body and the foundation rock for suitable load transfer from the dam body to the adjacent abutment. Also, a continuous joint has been provided between the dam body and Pulvino known as peripheral joint.

3.2. Transient thermal analysis

The finite element model of dam body consists of 1748 elements and 2120 nodes and has three layers in thickness (Figure 4(a)). Mainly, eight-node brick solid-thermal elements with one Degree Of thermal Freedom (DOF) are used for modeling while some prism elements are used in the main body-Pulvino connection (Figure 4(e)).

The closure (reference) temperature of 23°C is applied to all nodes of the body. Also, as mentioned before, air temperature is obtained from nearest station and the water temperature is computed using the empirical-analytical Bofang's relations. Figure 5 shows the air temperatures for six years in the dam site and also a comparison between the water temperatures recorded by thermometers and those computed by Bofang's method. As seen, the calculated reservoir water temperature is in good agreement with the recorded temperature in the considered elevation. Reservoir water level fluctuations are also shown in this figure.

In order to apply the solar radiation effects, the direct and indirect values of the daily radiation on the horizontal plane should be determined. Due to the lack of required instruments for measuring radiation near the dam site, its amount is determined according to the recorded daily sunshine hours at Dez Station for several years and calculated based on relations summarized in Figure 3. Direct, indirect and total radiation calculated for the years 1972 to 1977 are shown in Figure 6. The reflection coefficient is assumed to be 0.2 for the region surrounding the site and 0.3 for water surface. Also, the absorption coefficient for the body concrete is assumed to be 0.7 [26].

The thermal calibration is conducted by comparison of the calculated results with the actual values recorded by the thermometers for block no. 9, which is selected as the reference one. The calibration process is performed for about six years, 1972 to 1977, because there are comprehensive data from thermometers installed in block no. 9 working properly. Figure 7 shows the location of block no. 9 in dam and also the position of the thermometers through the thickness. Based on the sensitivity analyses on thermal analyses, the following properties are obtained for concrete: Thermal conductivity coefficient is 1.7 W/m°K, specific heat coefficient is 0.25 W/hr.kg°C, solar absorptivity coefficient is 0.7, emissivity coefficient of concrete surface is 0.8, and diffuse reflectance coefficients are 0.3 and 0.2 on upstream and downstream faces, respectively. The convection coefficients of air and water are assumed to be 60 and 6000 W/m^2°K, respectively. Figure 8 compares the results of the thermal calibration at different levels and sections with those recorded by the thermometers for the considered period of time at the reference block. Results confirm that the provided thermal model considering the solar radiation effects provides the responses which are in excellent agreement with the actual recorded data by the thermometers.

Figure 9 shows the temperature distribution on both the upstream and downstream faces of the dam for three months of 1973 considering/neglecting solar radiation effects. As seen, solar radiation has a crucial role in creation of non-uniform temperature distribution on the dam faces. It means, for example, the temperature differences between some coincident nodes highly affected by solar radiation is about 10°C for the hottest month. In the case of arch dams, especial geometry of the structure leads to heat concentration at some regions even in the same elevation. Due to the location of Dez Dam which is in north of the earth, and considering that the axis of the dam has a slight angle (about 6°) to the geographic south, the sun which is located in the southern glows to downstream face and leads to more heat concentration on the face near the abutments and middle elevations.

The effect of direct solar radiation is almost negligible on the upstream face because it is fully behind the sun. This distribution is affected by the indirect radiation reflected from the environmental surfaces,

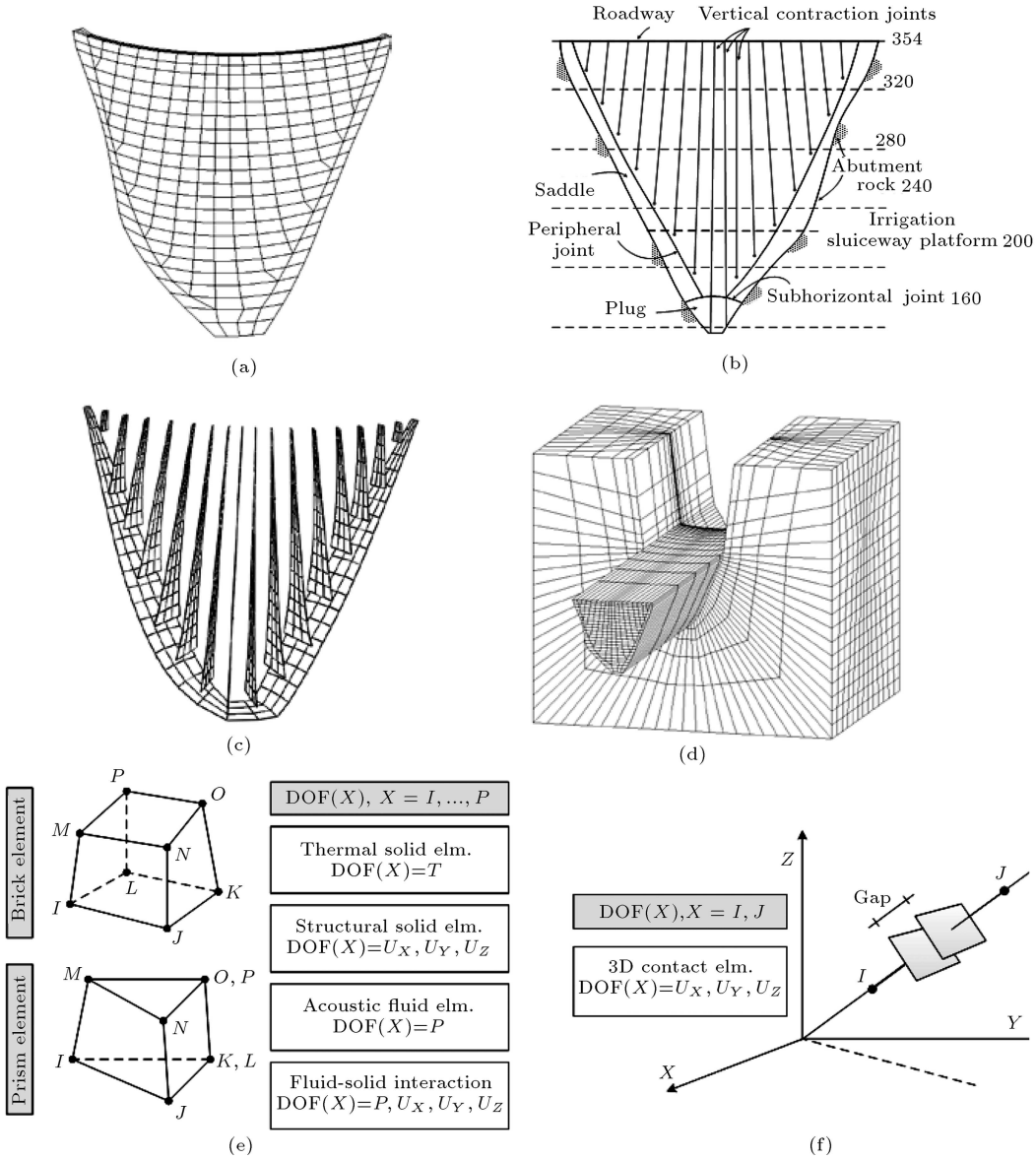

Figure 4. Finite element model: (a) Dam body; (b) downstream view and measure lines; (c) contraction and peripheral joints; (d) reservoir and foundation; (e) structural, acoustic and thermal elements; and (f) contact element.

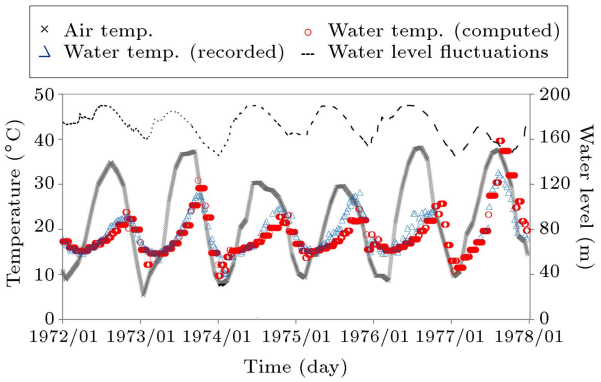

Figure 5. Time history of the air temperature, computed and recorded water temperature (for a thermometer installed in upstream face at the elevation 316.5 m), and water level variations for six years at Dez Dam site.

which is almost insignificant. The contours show the effects of reservoir level and water temperature on thermal distribution of the upstream face. Temperature variation is not considerable in the lower part of the dam, especially along the same elevation because the concrete in these regions is affected mostly by the reservoir temperature instead of the air temperature and the solar radiation.

3.3. Transient structural analysis

Figure 5(b) shows the downstream view of the dam including the measure lines [33]. Structural-solid elements are used for developing the finite element model for the transient structural analyses. The structural finite element model is similar to the thermal model while the structural-solid elements have

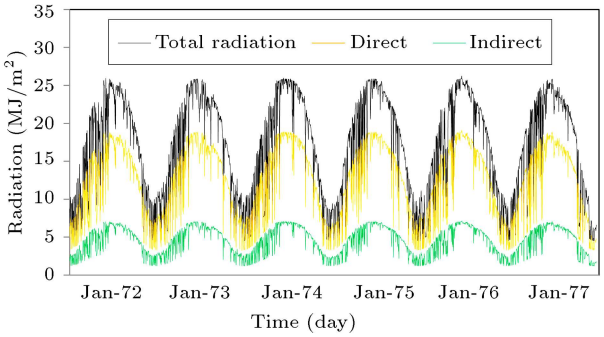

Figure 6. Calculated values for the direct, indirect and total radiation at the dam site.

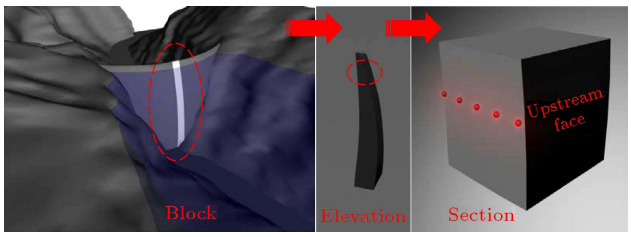

Figure 7. Location of the reference block and the thermometers position.

three translational DOFs at each node (Figure 4(e)). The compressible acoustic-fluid elements with three translational DOFs and one pressure DOF are used for modeling the reservoir water. The translational DOFs are only active on the dam-reservoir interface (Figure 4(e)). The total number of elements in dam, foundation and the reservoir are 792, 3770 and 3660, respectively (Figure 4(d)).

Also, 956 contact elements have been used for modeling the vertical and peripheral joints (Figure 4(c)). These 3D node-to-node contact elements have three DOFs at each node (Figure 4(f)) [34]. They support only the compression in the normal direction on the joint face and also shears in the tangential direction. The contact element cannot endure any tensile force or stress, but when it is in compression, it can support compression forces according to its normal stiffness coefficient and shear forces according to its tangential stiffness coefficient. When shear force resultant in the joint exceeds the joint sliding resisting force, the two nodes of the element begin sliding with respect to each other [34].

Foundation rock is assumed to be massless and all far-end nodes are restricted in three translational directions. The reservoir pressure at the free surface is assumed to be zero (surface sloshing is neglected due to the height of dam) [35]. The hydrodynamic waves are completely absorbed at the far-end reservoir boundary. Wave reflection coefficient applied on the bottom and sides of the reservoir medium is taken to be 0.8, conservatively [34]. The dynamic governing equations in the structure and reservoir media are solved simultaneously using unsymetric numerical methods [35].

Considering the reliability and accuracy of available 16 series of geodetic data obtained from micro geodesies measurement conducted on the dam site, series nos. 9, 10, 11 and 15 are selected for calibrating the numerical model. Figure 10 shows the results obtained from the last set of sensitivity analyses for the reference block. As seen, the responses of numerical model are in acceptable agreement with those obtained using geodetic measurement. Based on the conducted static calibration procedure, mechanical properties of concrete are obtained as: mass density is 2400 kg/m^3, modulus of elasticity is 40 GPa, Poisson's ratio is 0.2, thermal expansion coefficient is 6×10^{-6}1/°C, and

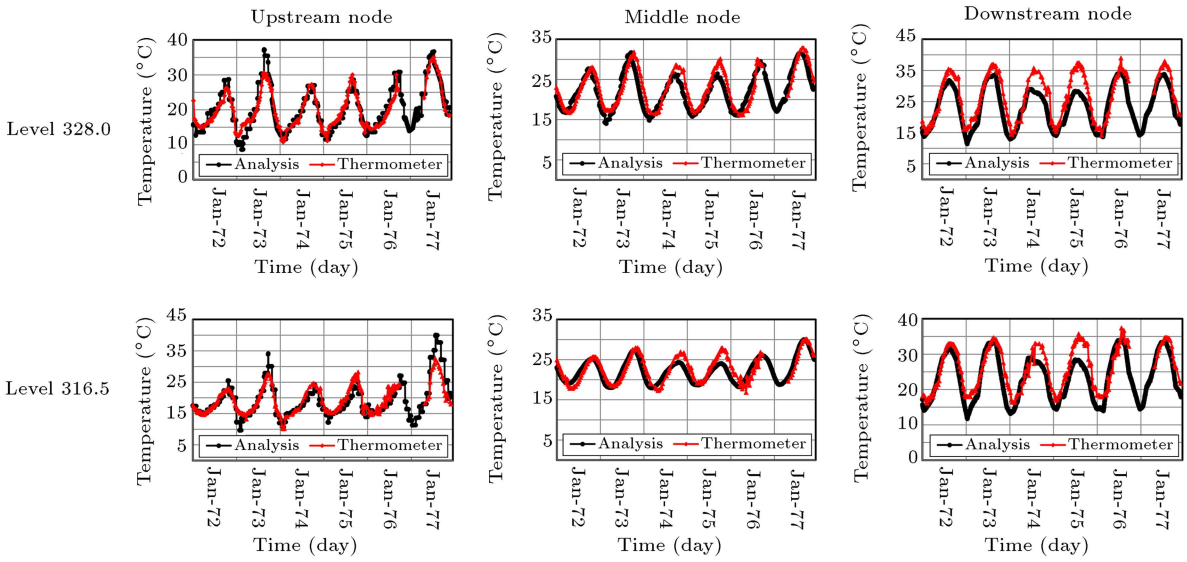

Figure 8. Comparison of the results obtained from thermal analysis and the thermometer records for the reference block [26].

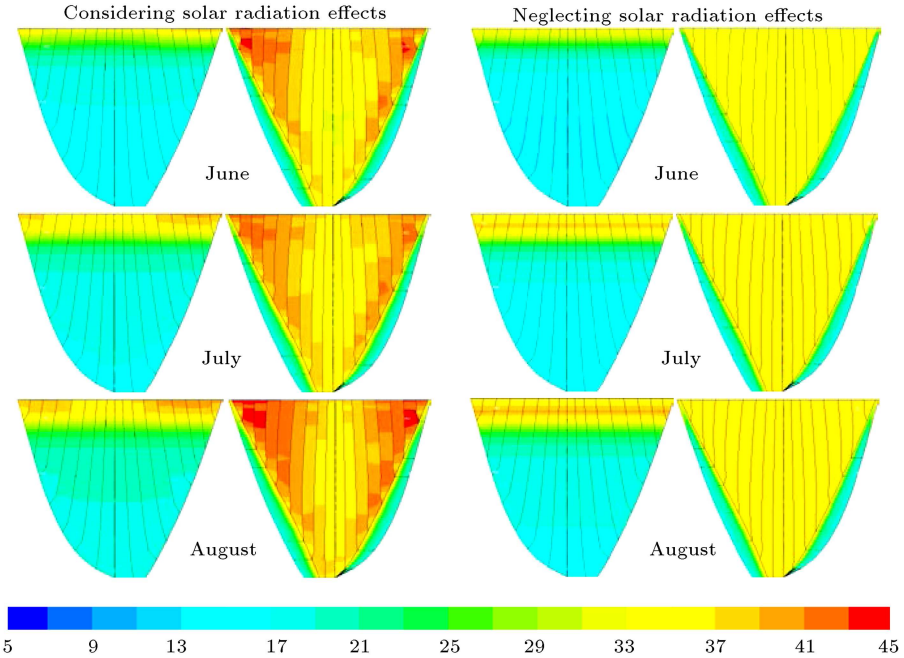

Figure 9. Temperature distribution on the upstream and downstream faces of the dam for three months of 1973, (°C) [26].

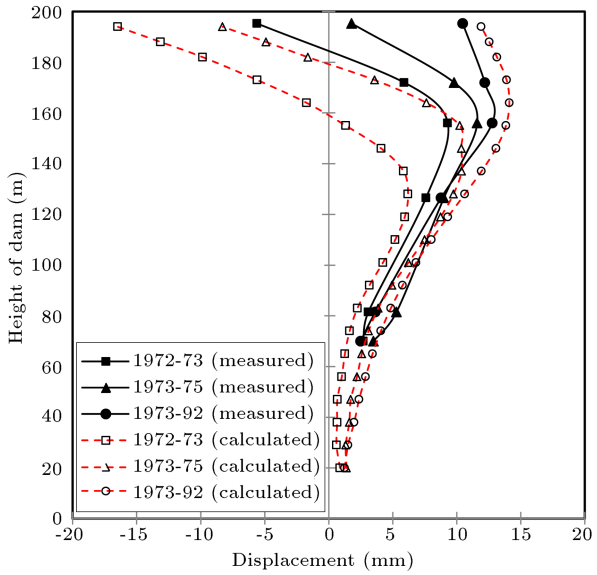

Figure 10. Comparison of the displacement in reference block between the numerical model and the geodetic measurements.

the grouting temperature is 23°C. Foundation rock deformation modulus in saturated and dry regions are 13 and 15 GPa, respectively, and the Poisson's ratio is 0.25.

Due to rate-dependence of mechanical and strength properties of concrete, the dynamic properties are different from static ones [36,37]. Dynamic modulus of elasticity and Poisson's ratio of concrete are 46 GPa and 0.14, respectively. Applied loads on the finite element models are the dam self-weight, hydrostatic pressure corresponding to summer or winter conditions, thermal loads (considering/neglecting the solar radiation effects) and finally, the seismic loads. Figure 11 summarizes all the required steps for uncoupled transient thermo-structural analysis of concrete dams. For the dynamic analysis, structural damping is applied to the equilibrium equations using Raighley method. A three-component earthquake ground motion which is consistent with the soil/rock type of the dam site should be used. Manjil ground motion at the Abbar Station is selected for this purpose [38]. The ground motion is scaled in Design Base Level (DBL) of dam site. The Peak Ground Accelerations (PGA) for the horizontal and vertical components are 0.24 g and 0.18 g, respectively. In order to reduce the computational efforts, only 11.5 s of the original acceleration time history corresponding to the strong ground motion of the record is applied to the coupled system. Damping for DBL excitation is assumed to be 5% of the critical damping.

Four different load combinations are used in this study to investigate the solar radiation effects. Table 1 summarizes the selected load combinations and the constituent loads as well. In order to find the critical load combination in each case, the critical date is recognized based on the thermal loads time histories considering the solar radiation effects.

Figure 12(a) and (b) show the non-concurrent envelope of the Maximum First Principal Stresses (MFPS) and Minimum Third Principal Stresses (MTPS) for both the upstream and downstream faces of the dam based on summer load combinations. MFPS considering and neglecting the solar radiation effects are 3.72 and 3.03 MPa, respectively. It means that,

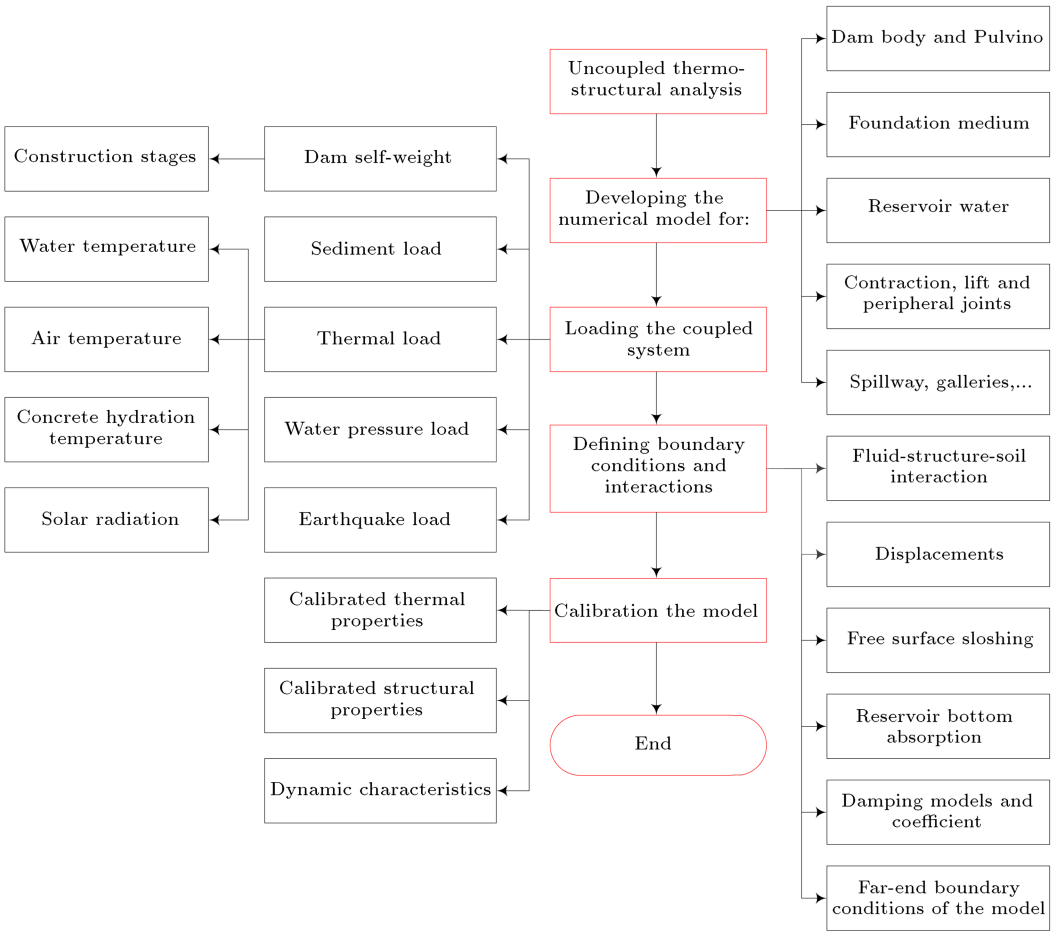

Figure 11. Performing uncoupled transient thermo-structural analysis on the dam-reservoir-foundation coupled system.

Table 1. Load combinations.

Load combo	Solar radiation effect	Thermal load	Hydrostatic load	Self-weight load	Seismic load
1	Yes	Summer	314.85m	Yes	DBE
2	No	Summer	314.85m	Yes	DBE
3	Yes	Winter	337.04m	Yes	DBE
4	No	Winter	337.04m	Yes	DBE

considering solar radiation increases tensile stresses about 22% for the selected ground motion. The location of MFPS is the same in both models. On the other hand, comparing MTPSs shows that considering solar radiation effects decrease compressive stresses from -11.5 to -10.7 MPa. The lower parts of the downstream face near the abutments and also some of central and upper parts of the upstream face experience higher compressive stresses. Also, solar radiation effect leads to the release of the compressive stresses in corner parts of the upstream face. It is noteworthy that the MFPS and MTPS in the dam without initial thermal load (for 314.85 m hydrostatic pressure load) are 2.45 and -13.87 MPa, respectively. Tensile and compressive strengths of concrete are 3.4 and 35 MPa, respectively [33]. Thus, neglecting the thermal stresses may leads to underestimation of the results.

Figure 13(a) compares displacement time histories of the crest point in the stream direction for load combinations (1) and (2). Under the current water level, the crest point shows 17 and 15 mm displacement in the downstream direction for the load combinations (1) and (2), respectively (displacements are due to hydrostatic pressure under gradually impounding the reservoir, dam self-weight under the staged construction, and the thermal loads). As it is clear, the general trend of the displacement time histories are close together; however, neglecting solar radiation effects increases displacement toward the upstream from 35 to 43 mm.

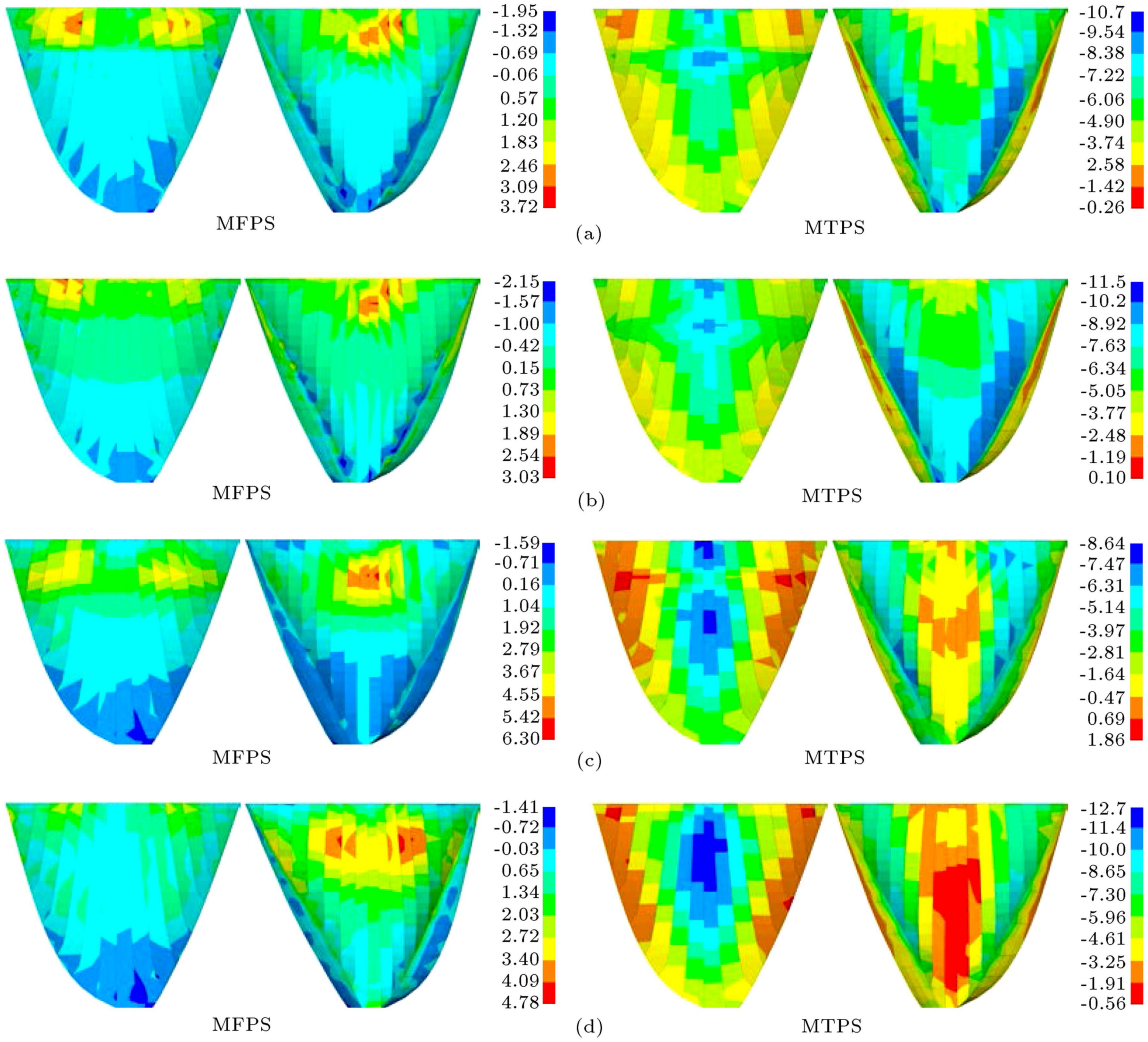

Figure 12. Non-concurrent envelope of MFPS and MTPS for (a) load combo 1, (b) load combo 2, (c) load combo 3, and (d) load combo 4 (MPa).

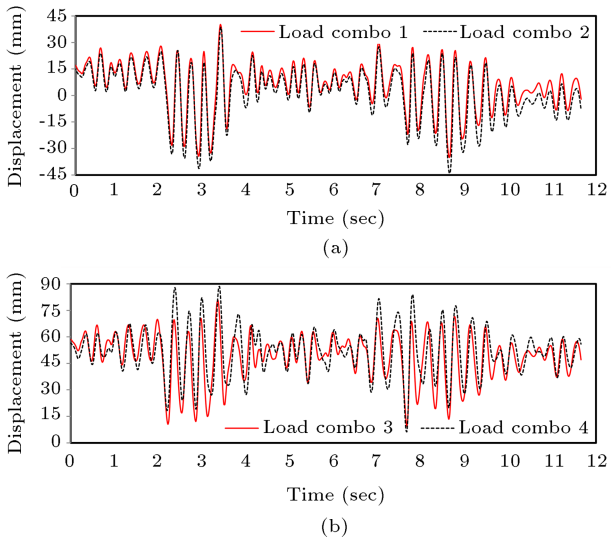

Figure 13. Displacement time history of the crest point in stream direction under (a) load combos 1 and 2, and (b) load combos 3 and 4.

Figure 12(c) and (d) show the non-concurrent envelope of MFPS and MTPS considering load combinations (3) and (4). In both cases winter temperatures are considered in conjunction with 337.04 m hydrostatic pressure load subjected to DBE. The values for MFPS considering and neglecting the solar radiation effects are 6.30 and 4.78 MPa, respectively. It shows that considering solar effects increase tensile stresses in the dam body. The location of MFPS is almost the same in both models. On the other hand, comparing MTPSs shows that considering solar radiation effects decrease compressive stresses from -12.7 to -8.64 MPa. The central and upper parts of the upstream face experience higher compressive stresses. The MFPS and MTPS in the dam without initial thermal load (for 337.04 m hydrostatic pressure load) are 3.85 and -15.12 MPa, respectively.

Figure 13(b) compares displacement time histories of the crest point in the stream direction for load combinations (3) and (4). Under the considered

hydrostatic load, the crest point experiences 57 and 56 mm displacement in the downstream direction for the cases considering/neglecting solar radiation, respectively. The larger value of the crest displacement in load combinations (3) and (4) rather than load combinations (1) and (2) can be attributed to the effects of joints opening/sliding under higher water pressure. Although the general trends of displacement time histories are close, neglecting solar radiation effects increases displacement toward the downstream from 84 to 89 mm, while both models have the same displacement toward the upstream direction.

4. Conclusion

In the present paper, the uncoupled transient thermo-structural response of a thin high arch dam is investigated using finite element technique. Thermal stresses are computed first in the dam using all the external thermal loads including solar radiation effect. Structural stresses are then computed based on dam body self-weight, hydrostatic pressure, and earthquake loads. Effects of all the contraction and peripheral joints are considered in terms of opening/closing between the dam blocks. Fluid-structure interaction is modeled using fluid finite elements. On the basis of the conducted thermo-structural analysis, the following conclusions can be drawn:

- Solar radiation leads to a non-uniform temperature distribution within dam body.
- Solar radiation mainly affects the downstream face of the dam. Temperature distribution on the upstream face especially in the lower parts of the body is mainly affected by the water temperature.
- Results of the thermal transient analysis considering the solar radiation effects are in good agreement with those recorded by the thermometers.
- In the both winter and summer load combinations, considering solar radiation increases tensile stresses and decreases compressive stresses under the selected ground motion.
- The locations of the maximum first principal stresses and minimum third principal stresses are the same for the models considering/neglecting solar radiation effects.
- Design of arch dams is mainly based on the generated tensile stresses in mass concrete. Thus, the effects of solar radiation should be considered in design process of thin high arch dams.

References

1. U.S. Army Corps of Engineering (USACE) "Arch dam design", Engineer Manual 1110-2-2201, Washington, DC, USA (1994).
2. Tarbox, G.S. "Design of concrete dams", In *Handbook of Dam Engineering*, Ed. A.R. Golze, Van Nostrand Reinhold Co. (1977).
3. ICOLD, *Deterioration of Dams and Reservoirs, Examples and Their Analysis*, A.A. Balkema Publishers Boorkfield, Vermont, USA (1984).
4. Ballivy, G., Benmokrane, B. and Chaallal, O. "Deformations generated in concrete under the influence of climatic conditions" [Deformations generees dans les betons sous l'influence des conditions climatiques], *Canadian Journal of Civil Engineering*, **18**, pp. 1088-1092 (1991).
5. Veltrop, J.A., Yeh, C.H. and Paul, W.J. "Evaluation of cracks in a multiple arch dam", *Dam Engineering*, **1**, pp. 5-12 (1990).
6. Tahmazian, B., Yeh, C.H. and Paul, W.J. "Thermal cracking and arch action in Daniel Johnson dam", *Proceedings of the International Symposium on Analytical Evaluation of Dam Related Safety Problems*, Copenhagen, Denmark, **1**, pp. 235-244 (1989).
7. NRC, *Earthquake Engineering for Concrete Dams, Design, Performance, and Research Needs*, National Academy Press, Washington, D.C., USA (1990).
8. Leger, P., Venturelli, J. and Bahattacharjee, S.S. "Seasonal temperature and stress distributions in concrete gravity dams, Part 1: Modeling", *Canadian Journal of Civil Engineering*, **20**, pp. 999-1017 (1993).
9. Meyer, T. and Mouvet, L. "Behavior analysis of the Vieux-Emosson arch-gravity dam under thermal loads", *Dam Engineering*, **VI**, pp. 275-292 (1995).
10. Agullo, L., Mirambell, E. and Aguado, A. "A model for the analysis of concrete dams due to environmental thermal effects", *International Journal of Numerical Methods for Heat and Fluid Flow*, **6**, pp. 25-36 (1996).
11. Zhang, Z. and Graga, V.K. "State of temperature and thermal stress in mass concrete structures subjected to thermal shock", *Dam Engineering*, **VIII**, pp. 336-350 (1996).
12. Chen, Y., Wang, C., Li, S., Wang, R. and He, J. "Simulation analysis of thermal stress of RCC dams using 3D finite element relocating mesh method", *Advanced in Engineering Software*, **32**, pp. 677-682 (2001).
13. Sheibany, F. and Ghaemian, M. "Effects of environmental action on thermal stress analysis of Karaj concrete arch dam", *Journal of Engineering Mechanics*, **132**, pp. 32-544 (2006).
14. Noorzaei, J., Bayagoob, K.H., Thanoon, W.A. and Jaafar, M.S. "Thermal and stress analysis of Kinta RCC dam", *Engineering Structures*, **28**, pp. 1795-1802 (2006).
15. Jaafar, M.S., Bayagoob, K.H., Noorzaei, J. and Thanoon, W.A. "Development of finite element computer code for thermal analysis of roller compacted

concrete dams", *Advances in Engineering Software*, **38**, pp. 886-895 (2007).

16. Leger, P. and Seydou, S. "Seasonal thermal displacements of gravity dams located in northern regions", *ASCE Journal of Performance of Constructed Facilities*, **23**, pp. 166-174 (2009).
17. Jin, F., Chen, Z., Wang, J. and Yang, J. "Practical procedure for predicting non-uniform temperature on the exposed face of arch dam", *Applied Thermal Engineering*, **30**, pp. 2146-2156 (2010).
18. Chen, S.H., Su, P.F. and Shahrour, I. "Composite element algorithm for the thermal analysis of mass concrete: Simulation of lift joint", *Finite Elements in Analysis and Design*, **47**, pp. 536-542 (2011).
19. Yang, J., Hu, Y., Zuo, Z., Jin, F. and Li, Q. "Thermal analysis of mass concrete embedded with double-layer staggered heterogeneous cooling water pipes", *Applied Thermal Engineering*, **35**, pp. 145-156 (2012).
20. Yangbo, L., Dahai, H. and Jianshu, O. "Fast algorithms of the simulation analysis of the thermal stresses on concrete dams during construction periods", *Physics Procedia*, **24**, pp. 1171-1177 (2012).
21. Fujun, C., Guohua, F., Xiaogang, M. and Zhinong, H. "Simulation analysis of crack cause of concrete overflow dam for Hadashan hydro project by 3D FEM", *Systems Engineering Procedia*, **3**, pp. 48-54 (2012).
22. Sabbagh-Yazdi, S.R. and Amiri-SaadatAbadi, T. "GFV solution on UTE mesh for transient modeling of concrete aging effects on thermal plane strains during construction of gravity dam", *Applied Mathematical Modeling*, **37**, pp. 82-101 (2013).
23. Kuzmanovic, V., Savic, L. and Mladenovic, N. "Computation of thermal-stresses and contraction joint distance of RCC dams", *Journal of Thermal Stresses*, **36**, pp. 112-134 (2013).
24. Hu, Y., Zuo, Z., Li, Q. and Duan, Y. "Boolean-based surface procedure for the external heat transfer analysis of dams during construction", *Mathematical Problems in Engineering*, Article ID 175616, DOI:10.1155/2013/175616 (2013).
25. Maken, D.D., Leger, P. and Roth, S.N. "Seasonal thermal cracking of concrete dams in northern regions", *ASCE Journal of Performance of Constructed Facilities*, **28**(4) (2014). DOI:10.1061/(ASCE)CF.1943-5509.0000483
26. Mirzabozorg, H., Hariri-Ardebili, M.A., Shirkhan, M. and Seyed-Kolbadi, S.M. "Mathematical modeling and numerical analysis of thermal distribution in arch dams considering solar radiation effect", *The Scientific World Journal*, Article ID 597393, 15 pages (2014).
27. Duffie, J.A. and Beckman, W.A., *Solar Engineering of Thermal Processes*, John Wiley and Sons Ltd., 2nd Ed. (1980).
28. Townsend, C.L. "Control of cracking in mass concrete structures", Engineering Monograph No. 34, U.S. Department of Interior, Bureau of Reclamation, Denver (1997).
29. Bofang, Z. "Predicting of water temperature in deep reservoirs", *Dam Engineering*, **VIII** (1997).
30. Angstrom, A. "Solar and terrestrial radiation", *Quarterly Journal of the Royal Meteorological Society*, **50**, pp. 121-125 (1924).
31. Hutton, D.V., *Fundamental of Finite Element Analysis*, Elizabeth A. Jonse Ltd., First Edition (2004).
32. Hariri-Ardebili, M.A., Mirzabozorg, H., Ghaemian, M., Akhavan, M. and Amini, R. "Calibration of 3D FE model of Dez high arch dam in thermal and static conditions using instruments and site observation", *Proceeding of the 6th International Conference in Dam Engineering*, Lisbon, Portugal (2011).
33. Hariri-Ardebili, M.A., Mirzabozorg, H. and Ghaemian, M. "Pulvino and peripheral joint effects on static and seismic safety of concrete arch dams", *Scientia Iranica, Transactions A: Civil Engineering*, **20**, pp. 1579-1594 (2013).
34. Hariri-Ardebili, M.A. and Kianoush, M.R. "Seismic analysis of a coupled dam-reservoir-foundation system considering pressure effects at opened joints", *Structure and Infrastructure Engineering*, **11**(7), pp. 833-850 (2015). DOI: 10.1080/15732479.2014.915857
35. Hariri-Ardebili, M.A. and Mirzabozorg, H. "A comparative study of the seismic stability of coupled arch dam-foundation-reservoir systems using infinite elements and viscous boundary models", *International Journal of Structural Stability and Dynamic*, **13**, 24 pages, DOI:10.1142/S0219455413500326 (2013).
36. FERC, "Engineering Guidelines for the Evaluation of Hydropower Projects- Chapter 11: Arch Dams", Federal Energy Regulatory Commission (Division of Dam Safety and Inspections), Washington, DC (1999).
37. U.S. Army Corps of Engineering (USACE) "Earthquake design and evaluation of concrete hydraulic structures", EM 1110-2-6053, Washington D.C., USA (2007).
38. PEER ground motion database, Beta version, University of California, Berkeley, CA, USA (2010). http://peer.berkeley.edu/peer_ground_motion_database,

Biographies

Hasan Mirzabozorg is Associate Professor of Civil Engineering at K.N. Toosi University of Technology, Tehran, Iran. His research interests are mainly nonlinear seismic analysis of concrete dams, fluid-structure interaction, concrete fracture mechanics, alkali-aggregate reaction and numerical methods in structural engineering.

Mohammad Amin Hariri-Ardebili is Post-Doctoral Research Associate at the University of Col-

orado, Boulder, USA. His research interests are concrete dam engineering, performance-based engineering, coupled system mechanics, mathematical modeling of alkali-silica reaction, and aging studies in nuclear power planes.

Meisam Shirkhan is a graduate student at K.N. Toosi University of Technology, Tehran, Iran. His research interests are finite element modeling, thermal analysis, dam engineering, and mathematical modeling of engineering problems.